vite by volume. Studies of natural samples suggest that mantle clinopyroxene may be able to incorporate an order of magnitude more hydrogen in its structure than can mantle garnet (*1*, *2*) and stishovite. Water can dissolve in slab clinopyroxene from the dehydration of hydrous minerals, which may be stable to depths of at least 100 km (*16*). When the hydrous pyroxene breaks down, some of the released water is incorporated in the crystallizing stishovite. In the transition zone, the garnet exsolves $CaSiO_3$ perovskite and eventually disappears (*15*). However, the stishovite, and its incorporated hydrogen, may remain stable if the slab sinks into the lower mantle.

The stability of stishovite is not limited to subduction zone conditions. Our OH-bearing samples were synthesized at 1200°C, more than 100° higher than the highest probable thermal stability of dense hydrous magnesium silicates at 10 GPa (*17*). Therefore, stishovite could store water in hot regions of the mantle as well as in cold subduction zones where these silicates might be stable.

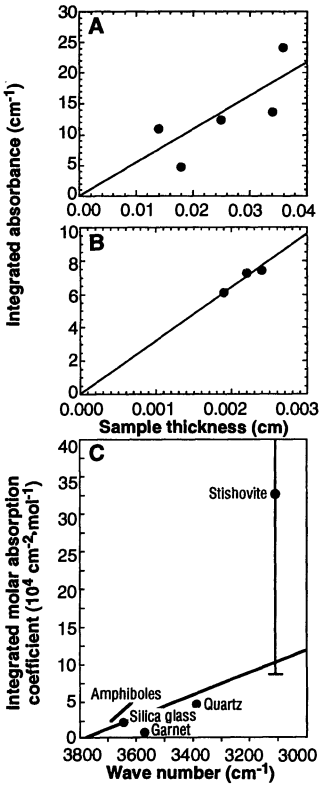

Fig. 3. Integrated absorbance of the IR band at 3111 cm^{-1} as a function of sample thickness in (**A**) polarized spectra of H-stishovite and (**B**) unpolarized Al-stishovite spectra. Lines represent the linear regression fits to the data, constrained to pass through the origin. The absence of systematic deviations of the data away from these lines suggests that they represent equilibrium values of H concentration. Before its use in Eq. 1, *A*/*d* for Al-stishovite must be multiplied by 2 to account for the fact that the Al-stishovite spectra are unpolarized (*13*); $A/d = 545 \pm 183$ cm^{-2} for (A) and 3201 ± 133 cm^{-2} for (B). (**C**) Integrated molar absorption coefficients of OH-stretching bands in various minerals and glasses as a function of wave number, recalculated for all OH groups oriented parallel to the electric vector of the radiation (*I* for stishovite has been multiplied by 2) (*13*). The solid line is the calibration of Paterson (*13*) for various minerals, glasses, and forms of water, including the silica glass and quartz points shown. The amphibole data are a least squares fit to eight data points (*14*); the garnet data are from (*2*).

REFERENCES AND NOTES

1. J. R. Smyth, D. R. Bell, G. R. Rossman, *Nature* **351**, 732 (1991).
2. D. R. Bell and G. R. Rossman, *Contrib. Mineral. Petrol.* **111**, 161 (1992).
3. R. J. Swope and J. R. Smyth, *Eos* **73**, 651 (1992).
4. P. F. McMillan, M. Akaogi, R. K. Sato, B. Poe, J. Foley, *Am. Mineral.* **76**, 354 (1991).
5. G. R. Rossman and J. R. Smyth, *ibid.* **75**, 775 (1990).
6. D. Walker, M. A. Carpenter, C. M. Hitch, *ibid.*, p. 1020. Experimental procedures were based on those of D. Walker [*ibid.* **76**, 1092 (1991)]. For each experiment, 10 to 15 mg of sample was sealed in a platinum capsule; experiments lasted for 2 hours.
7. We used a Digilab (Cambridge, MA) FTS-40 micro-IR instrument. Spectra were obtained of five crystals of H-stishovite (140 to 360 μm thick; sample 1), two of D-stishovite (160 and 310 μm thick), and three of Al-stishovite (19 to 24 μm thick; sample 6).
8. The expected value is 1.37. The observed ratio is lower because of anharmonicity of the O–H bond.
9. C. Meade and E. Ito, *Eos* **74**, 314 (1993).
10. K. Nakamoto, M. Margoshes, R. E. Rundle, *J. Am. Chem. Soc.* **77**, 6480 (1955).
11. Background H counts are around 50,000 H per 10^6 Si, which is four orders of magnitude higher than background D counts.
12. The 2σ error was calculated from the uncertainties in the SIMS measurement of D concentration and FTIR determination of *A*/*d*. Using Eq. 1 we also calculated a value of *I* for D-stishovite of 39,000 liters·cm^{-2}·mol^{-1}. We expect the molar absorptivity for the heavier isotope to be smaller [E. B. Wilson, J. C. Decius, P. C. Cross, *Molecular Vibrations* (McGraw-Hill, New York, 1955)]. Infrared measurements on H- and D-bearing rhyolite glasses have shown that $A'/d_{OD} \div A'/d_{OH} = \sim 0.56$, where A' is the IR peak height [T. Stanton, thesis, Arizona State University (1989)]. Our measurements, $A'/d = 15.3 \pm 4.6$ cm^{-1} for H-stishovite and $A'/d = 6.3 \pm 0.4$ cm^{-1} for D-stishovite, are in close agreement with the previous results.
13. M. S. Paterson, *Bull. Mineral.* **105**, 20 (1982).
14. H. Skogby and G. R. Rossman, *Phys. Chem. Miner.* **18**, 64 (1991).
15. T. Irifune and A. E. Ringwood, in *High-Pressure Research in Mineral Physics*, M. H. Manghnani and Y. Syono, Eds. (American Geophysical Union, Washington, DC, 1987), pp. 231–242.
16. A. R. Pawley and J. R. Holloway, *Science* **260**, 664 (1993).
17. A. B. Thompson, *Nature* **358**, 295 (1992).
18. All bulk compositions except for sample 7 consisted of mixtures of SiO_2 glass, Al_2O_3, and distilled water. Sample 7 is a natural pyrophyllite sample containing 0.46% Fe_2O_3. Compositions of samples 1 and 2 were measured by SIMS with a Cameca (Stamford, CT) IMS 3f ion microprobe. Compositions of samples 5 to 8 were measured by EMPA with a JEOL (Peabody, MA) Model JXA 8600 electron microprobe: average Al_2O_3 content was 1.51% by weight (17,800 atomic ppm Al). No elements other than those quoted were detected by either technique.
19. We thank R. Hervig for assistance and advice with SIMS analysis. Supported by Arizona State University (multianvil facility) and National Science Foundation grants EAR 9205061, EAR 8408163 (electron microprobe facility), and EAR 8915759 (FTIR facility).

23 March 1993; accepted 22 June 1993

A Two-Tiered Approach to Long-Range Climate Forecasting

L. Bengtsson, U. Schlese, E. Roeckner, M. Latif, T. P. Barnett,* N. Graham

Long-range global climate forecasts were made by use of a model for predicting a tropical Pacific sea-surface temperature (SST) in tandem with an atmospheric general circulation model. The SST is predicted first at long lead times into the future. These ocean forecasts are then used to force the atmospheric model and so produce climate forecasts at lead times of the SST forecasts. Prediction of seven large climatic events of the 1970s to 1990s by this technique are in good agreement with observations over many regions of the globe.

Useful climate predictions have heretofore been made largely by empirical techniques. The physical processes responsible for any forecast skill that these methods may exhibit are often not clear. Furthermore, these methods are impossible to apply over the data-sparse regions that make up most of the planetary surface.

In this report, we describe the development and partial testing of a long-range climate forecast method that is largely based on physical principles and that appears to have predictive skill over large areas of the world. The first phase of the two-part technique uses a simplified coupled ocean-atmosphere model to forecast, two seasons in advance, tropical Pacific SSTs during the northern winter, that is, essentially El Niño–Southern Oscillation (ENSO) events, which are known to affect

L. Bengtsson, U. Schlese, E. Roeckner, M. Latif, Max-Planck-Institut für Meteorologie, Hamburg, Germany.
T. P. Barnett and N. Graham, Scripps Institution of Oceanography, University of California at San Diego, La Jolla, CA 92093.
*To whom correspondence should be addressed.

climate anomalies for a large part of the Earth. The predicted winter SST fields are then used to force an atmosphere climate model, the output from which constitutes a forecast two seasons in advance of winter climate conditions over the globe.

The capability to forecast some atmospheric climate changes a season or more in advance has been demonstrated by a variety of statistical forecasting techniques (*1*, *2*). The source of this predictive skill has been traced to low-frequency changes in the SST of the oceans, particularly the tropical Pacific Ocean. Atmospheric general circulation models (AGCMs) reproduce well the variability of the large-scale circulation, including precipitation and surface temperature anomalies, provided they are forced with observed SST; that is, they have skill at "nowcasting" (*3*, *4*). But their skill at long-range climate forecasting does not match that of the statistical techniques if the AGCMs are used in a stand-alone mode because the memory of the climate system resides mainly in the ocean, not the atmosphere. Considerable efforts are now being directed toward developing forecasting systems in which comprehensive AGCMs are coupled to ocean models to produce coupled GCMs (CGCMs) in an attempt to provide ocean memory and evolution required for successful long-range forecasts. Although promising work is under way, these CGCMs have, to date, showed limited forecast skill because of a variety of complex problems. The main problem is difficulties in the physical coupling of the two systems; this coupling requires an accuracy in flux determination between the two media that has not yet been achieved (*5*).

The above situation for atmospheric forecasting is in marked contrast to the current state of our ability to forecast temperature changes in the tropical Pacific Ocean associated with ENSO (*2*, *6*, *7*). Skillful forecasts of tropical SSTs out to lead times of 12 to 18 months for substantial warm or cold events have been demonstrated by widely different techniques. However, these ocean forecast tools by themselves are of little use for predicting atmospheric changes outside of a narrow equatorial Pacific strip. Yet it is well known that there is a close simultaneous relation between changes in SST in the central equatorial Pacific and various atmospheric variables over many regions of the world.

Our experimental procedure was to use a hybrid coupled model (HCM) for the long-range tropical Pacific SST forecasts (*7*). This model consisted of a statistical atmosphere derived from data driven by SST coupled to a fully nonlinear ocean general circulation model of the tropical Pacific driven by wind stress (*4*, *8*). The HCM performs best during the northern winter and has demonstrated forecast skill out to lead times of 18 months. The model is spun up to 1 June of the forecast

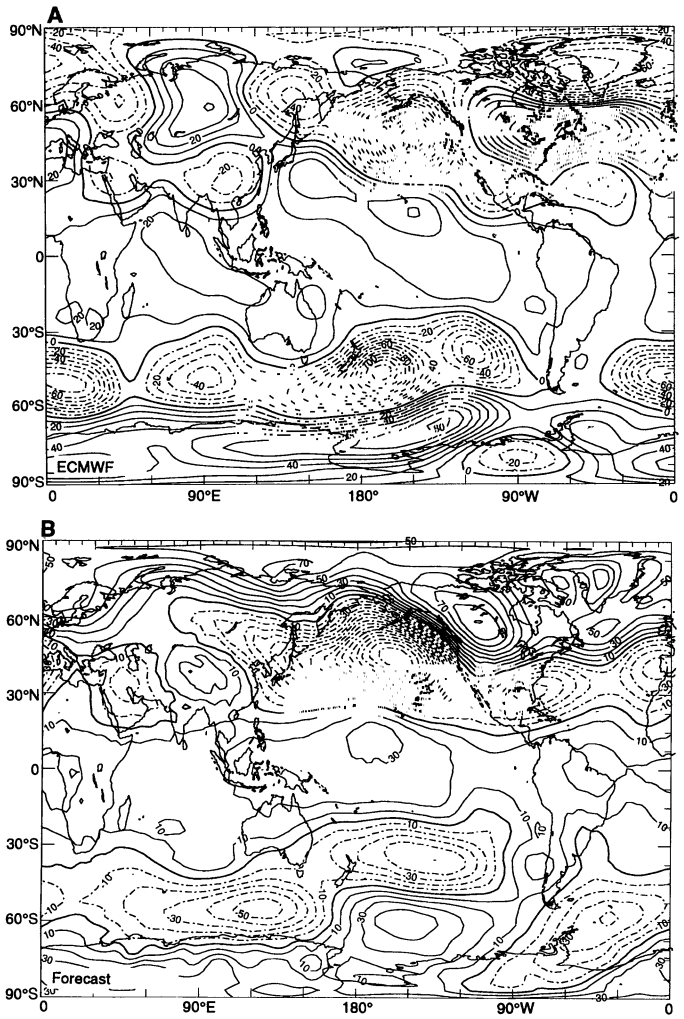

Fig. 1. Observed (**A**) and predicted (**B**) 500-mbar height anomaly fields (geopotential meters) for the warm event of the northern winter of 1982 to 1983. The observations are from the analyzed product of the ECMWF, and the forecasts, made at a lead time of 6 to 8 months, are from the climate forecast technique described in the text. Solid contours are associated with positive height anomalies, and dashed lines go with lower than normal heights.

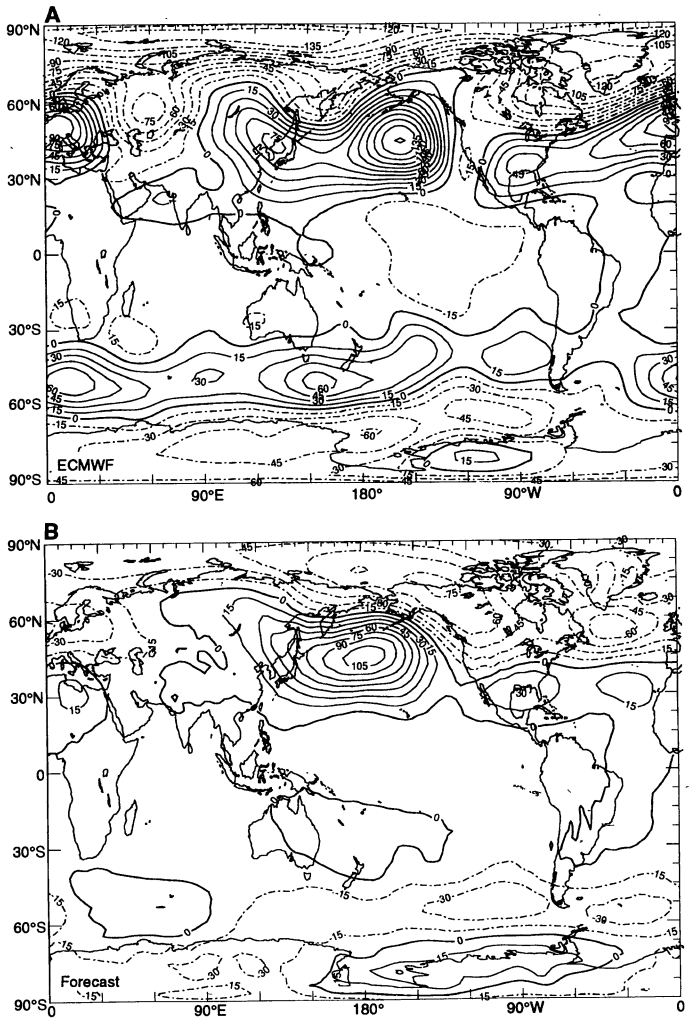

Fig. 2. Same as Fig. 1 but for the cold event of the northern winter of 1988 to 1989.

year by wind stress produced by forcing the atmospheric component of the HCM with observed SST. The HCM is then allowed to produce predictions for the entire tropical Pacific Ocean in its fully coupled mode.

The model we used to produce the atmospheric nowcasts from the SST forecasts is the T42 version of the Max-Planck-Institut für Meteorologie (Hamburg) climate model (ECHAM3) (9). This AGCM has 19 levels in the vertical and a horizontal resolution of approximately 2.5° of longitude by 2.5° of latitude. In this set of experiments, we prescribed the seasonal cycle of solar radiation and sea ice variation. The HCM-predicted SSTs were fed to the AGCM for the tropical Pacific only. In the remainder of the ocean, SST is prescribed to follow climatology. All other variables in the AGCM are computed during the course of the integration.

Seven particular ENSO winters were chosen as forecast targets. The target years consisted of three cold events (1970 to 1971, 1973 to 1974, and 1988 to 1989) and four warm events (1972 to 1973, 1982 to 1983, 1986 to 1987, and 1991 to 1992). These events constitute large climatic signals, and, if the HCM or ECHAM3 could not produce useful forecasts for these years, then our approach likely would not work.

The AGCM integrations were started on 1 October of the forecast year from an initial condition provided by a control run. This procedure was intended to allow the atmospheric model to spin up before forecasting the months of interest (December, January, and February). The predicted SST fields were interpolated in time to match the evolution of time in the ECHAM3. The atmospheric model integration was continued through February of the subsequent year. The AGCM outputs for a number of observable variables were saved as monthly averages. Because we expected some noise in the forecasts, especially for the higher latitudes, we repeated the AGCM forecasts for each year three times using a different 1 October initial condition for each forecast. Thus, for each forecast year, we had three realizations of a forecast for the selected winter. The total months of forecast for each field amounted to 63: seven different years times three different months times three different realizations of each forecast.

Only a few homogeneous sets of observations can be used for the evaluation of the forecasts in a systematic manner. With this in mind and given the volume of forecast fields, we present here the forecast results of two of the largest forecast events for which there are reliable verification data. The skill of these forecasts was evaluated on a global basis by comparison with the European Centre for Medium Range Forecasting (ECMWF) fields of 500-mbar height (a critical atmospheric variable). These comparisons (Figs. 1 and 2) are in accord with those obtained when the entire set of forecasts was compared in the Northern Hemisphere north of about 20°N with an existing set of observed 700-mbar height data from the National Meteorological Center.

Perhaps the largest warm ENSO event of this century occurred during the winter of 1982 to 1983. The correspondence between the observed anomalies in the 500-mbar height field for that winter and the anomalous

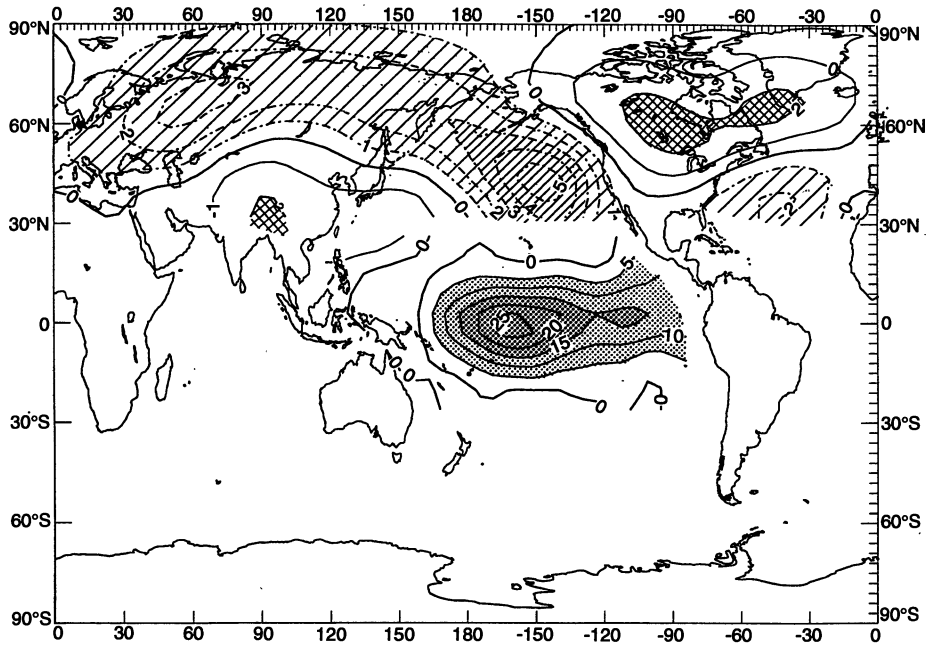

Fig. 3. The statistical relation between tropical SST anomalies (heavy stippled region) and corresponding 700-mbar height anomalies (hatched and checkered areas) obtained from observations; values are statistical weights. Similar patterns are obtained from the ECHAM3 model forced by observed SSTs.

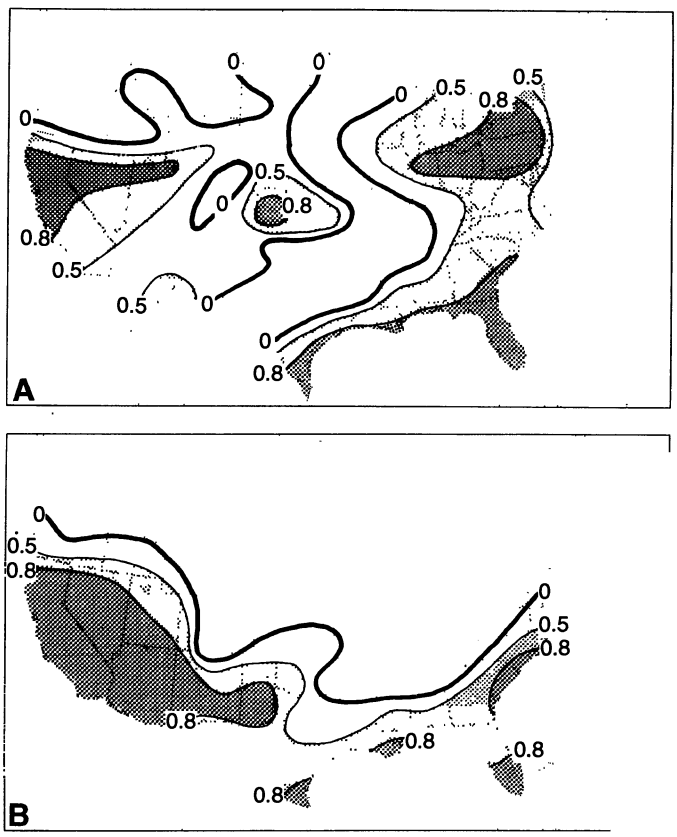

Fig. 4. (**A**) Correlation between forecasts with a two-season lead time of winter precipitation for six large ENSO events and observations. (**B**) Correlation between observed central Pacific winter SST anomalies for the same six events and contemporaneously observed precipitation. The forecast beats the nowcast over much of the United States.

height field averaged over the three forecasts obtained from our technique at lead times of 6 to 8 months is good (Fig. 1) in selected regions of the globe, particularly the tropical oceans and land masses and the northern Pacific Ocean (Aleutian Low). The forecast is moderately good in the mid-latitude of the Southern Hemisphere and over much of North America and central Eurasia. The forecasts are quite poor over Europe, eastern North America, and Southeast Asia. However, in balance, the forecast with a 6-month lead time captured many of the major atmospheric anomalies of the remarkable winter of 1982 to 1983.

The largest cold ENSO event observed in the last 20 years occurred in the winter of 1988 to 1989. The forecast for this winter (Fig. 2) successfully captured the weakening of the Aleutian Low, the intensification of the ridge over the United States and the Atlantic, and the deepening of the Icelandic Low. As with the forecast for the warm ENSO event, this forecast is poor over Europe and much of Asia. The tropics are only moderately well depicted; the largest failing is in the central equatorial Pacific where the observations show a weak negative anomaly (an association one would not expect on the basis of numerous empirical studies).

Are these forecast results fortuitous or genuine? A detailed statistical evaluation of the forecasts by a Monte Carlo technique shows that the skill of the model in much of the tropics and central North Pacific has significance levels of 0.05 or better, whereas the skill of the model in regions of moderately good forecasts noted above has significance levels of 0.10. Another type of evaluation is to compute the simultaneous wintertime relation between tropical SST and 700-mbar height (*10*). The results (Fig. 3) show that the best relation between the variables is associated with warm or cold SST anomalies in the central equatorial Pacific and lower or higher than normal heights in the central Pacific, eastern Asia, and the subtropical Atlantic, whereas pressure in most of North America and southern Asia was higher or lower than normal. A comparison of Figs. 1 and 3 shows that the forecast is good in just the regions that one would expect from the empirical studies. Reversing the signs of the anomalies on Fig. 3, to represent a cold event situation, gives the same conclusions. Data for the Southern Hemisphere are not adequate to establish a similar empirical comparison.

The above result raises a final question: Why not use a statistical model in place of the AGCM and the forecast SST in a much simpler two-tiered forecast scheme? There are two clear answers to this question. (i) In many parts of the world the data are not adequate to construct such statistical models. Thus, the scheme presented here, or something like it, is the only hope for long-range climate forecasts in these data-sparse regions. (ii) Complex, highly nonlinear climate variables such as precipitation are not very amenable to statistical forecasting. This is illustrated in Fig. 4 where the correlation between forecast precipitation by our approach and observation is compared with the correlation between simultaneously observed winter SST and precipitation, the latter being a nowcast. This is clearly an unfair test for our forecast scheme. But the nowcast is only slightly better than the forecast with a two-season lead time in the southwestern United States. The forecast is slightly better in the southeastern region. Most important, the forecast has skill over the eastern third of the nation whereas the nowcast has none. We conclude that our approach carries skill not likely to be found in a purely statistical competitor.

The forecast skills described above suggest that our approach can provide highly useful predictions of climatic anomalies associated with ENSO events during the northern winter for lead times of at least 6 months. The success of the method relies on the prediction and occurrence of a significant warm or cold event. Such events occur every 2 to 4 years, so we do not expect our method to give reliable predictions every year. But the largest events tend to have the largest societal impact, and those appear amenable to our approach.

REFERENCES AND NOTES

1. T. P. Barnett, *Mon. Weather Rev.* **109**, 1021 (1981); A. Broccoli and R. Harnack, *ibid.*, p. 2107; T. P. Barnett and R. W. Preisendorfer, *J. Atmos. Sci.* **35**, 1771 (1978); *Mon. Weather Rev.* **115**, 1825 (1987); R. Harnack, J. Harnack, J. Lanzante, *ibid.* **114**, 1950 (1986).
2. T. P. Barnett, *J. Phys. Oceanogr.* **11**, 1043 (1981).
3. J. Shukla and J. M. Wallace, *J. Atmos. Sci.* **40**, 1613 (1983); M. Latif, J. Biercamp, H. von Storch, M. J. McPhaden, E. Kirk, *J. Clim.* **3**, 509 (1990); N. C. Lau and M. Nath, *ibid.*, p. 965; K. Arpe, L. Bengtsson, E. Roeckner, in preparation.
4. T. P. Barnett, E. Kirk, M. Latif, E. Roeckner, *J. Clim.* **4**, 487 (1991).
5. D. Neelin *et al.*, *Clim. Dyn.* **7**, 73 (1992); K. Miyakoda, A. Rosati, R. Gudgel, *Global Climate Change* (*NATO Advanced Study Institute Series*, Springer-Verlag, Berlin, 1993); K. Miyakoda, J. Sirutis, A. Rosati, R. Gudgel, in *Proceedings of the Workshop on Japanese-Coupled Ocean Atmosphere Response Experiments* (Meteorology Research Report, Geophysics Institute, University of Tokyo, Tokyo, 1989), p. 93; K. Miyakoda, J. Sirutis, A. Rosati, J. Derber, in *Proceedings of U.S.–PRC International Tropical Oceans and Global Atmosphere Project (TOGA) Symposium*, C. Jiping and J. Young, Eds. (China Ocean Press, Beijing, 1988), p. 417.
6. M. A. Cane and S. E. Zebiak, *Science* **228**, 1085 (1985); N. E. Graham, J. Michaelsen, T. P. Barnett, *J. Geophys. Res.* **92**, 14271 (1987); S. Zebiak and M. Cane, *Mon. Weather Rev.* **115**, 2262 (1987); T. Barnett *et al.*, *Science* **241**, 192 (1988).
7. T. P. Barnett, N. Graham, M. Latif, S. Pazan, W. White, *J. Clim.*, in press.
8. M. Latif, *J. Phys. Oceanogr.* **17**, 246 (1987).
9. E. Roeckner *et al.*, *Max-Planck-Inst. Meteorol. Rep. No. 93* (October 1992).
10. N. E. Graham, *Clim. Dyn.*, in press; patterns shown in Fig. 3 are for 19 years of observations, 1970 to 1989.

11. This work was supported by National Science Foundation grant ATM88-14571 and National Oceanic and Atmospheric Administration grant NA26GP0078-01 under the TOGA Program of Prediction.

6 April 1993; accepted 8 June 1993

A Solid Sulfur Cathode for Aqueous Batteries

Dharmasena Peramunage and Stuart Licht*

Because of its high resistivity and subsequent low electroactivity, sulfur is not normally considered a room-temperature battery cathode. An elemental sulfur cathode has been made with a measured capacity of over 900 ampere·hours per kilogram, more than 90 percent of the theoretical storage capacity of solid sulfur at room temperature, accessed by means of a lightweight, highly conductive, aqueous polysulfide interface through the electrocatalyzed reaction $S + H_2O + 2e^- \rightarrow HS^- + OH^-$. This solid sulfur cathode was first used in a battery with an aluminum anode for an overall discharge reaction $2Al + 3S + 3OH^- + 3H_2O \rightarrow 2Al(OH)_3 + 3HS^-$, giving a cell potential of 1.3 volts. The theoretical specific energy of the aluminum-sulfur battery (based on potassium salts) is 910 watt·hours per kilogram with an experimental specific energy of up to 220 watt·hours per kilogram.

There is a critical need for new electrochemical storage concepts that address future societal needs for consumer batteries and the propulsion of electric vehicles (*1*, *2*). The search for contemporary batteries has blurred the conventional distinctions of electrochemical storage systems. For example, candidates for electrochemical propulsion include mechanically rechargeable primary batteries, secondary batteries, and fuel cells (*2*). There has been considerable interest in nonaqueous electrolytes (such as chloroaluminate), ambient-temperature molten

Department of Chemistry, Clark University, Worcester, MA 01610.
*To whom correspondence should be addressed.